AGU ADVANCING EARTH AND SPACE SCIENCE

JGR Oceans

RESEARCH ARTICLE

10.1029/2020JC016964

Key Points:

- A rapid cooling event over the western Pacific region during the Middle Bronze Age was identified
- The cooling event recorded in coral archives broadly agrees with those in foraminiferal and stalagmite records
- The rapid cooling and drying process in inland China might have led to the collapse of the Xia Dynasty

Supporting Information:

- Supporting Information S1

Correspondence to:
W. Deng,
wfdeng@gig.ac.cn

Citation:
Xiao, H., Deng, W., Liu, X., Chen, X., Guo, Y., Zhao, J., et al. (2021). A rapid cooling event over the western Pacific region during the Middle Bronze Age. *Journal of Geophysical Research: Oceans*, *126*, e2020JC016964. https://doi.org/10.1029/2020JC016964

Received 9 NOV 2020
Accepted 10 DEC 2020

A Rapid Cooling Event Over the Western Pacific Region During the Middle Bronze Age

Hangfang Xiao[1,2], Wenfeng Deng[1,3], Xi Liu[1,3], Xuefei Chen[1,3], Yangrui Guo[1,3], Jian-xin Zhao[4], Ti Zeng[3,5], and Gangjian Wei[1,3]

[1]State Key Laboratory of Isotope Geochemistry, Guangzhou Institute of Geochemistry, Chinese Academy of Sciences, Guangzhou, China, [2]College of Earth and Planetary Sciences, University of Chinese Academy of Sciences, Beijing, China, [3]Southern Marine Science and Engineering Guangdong Laboratory, Guangzhou, China, [4]School of Earth and Environmental Sciences, Radiogenic Isotope Facility, The University of Queensland, Brisbane, Queensland, Australia, [5]Key Laboratory of Marginal Sea Geology, Guangzhou Institute of Geochemistry, Chinese Academy of Sciences, Guangzhou, China

Abstract Climate change in the mid-to-late Holocene transition is very important for predicting future climate trends and understanding the relationship between abrupt climate change and the development of past human civilization. In this study, Sr/Ca ratios and $\delta^{18}O$ records with the annual resolution extracted from four fossil corals that were growing during the Middle Bronze Age Cold Epoch (MBACE) were used to reconstruct sea surface temperature (SST) and seawater $\delta^{18}O$ ($\delta^{18}O_{sw}$) in the South China Sea (SCS) during the mid-to-late Holocene transition. The results indicate that the SCS experienced a rapid cooling and wetting event during the period of ∼3,500–3,800 years BP (before present year 1950). Specifically, the average SST and $\delta^{18}O_{sw}$ declined rapidly by ∼3°C and ∼0.65‰, respectively, over an interval of ∼100 years from ∼3,850 years BP to ∼3,750 years BP. This rapid climate change pattern recorded in coral archives broadly agrees with those in foraminiferal and stalagmite records from adjacent land and ocean areas. Consistent with other records from the North Atlantic, this cold event in the Asia-Western Pacific region that occurred during the MBACE and was originally identified in the North Atlantic and European regions should have occurred at the global scale, which might be caused by changes in the Asian summer monsoon linked with solar irradiance and/or the North Atlantic climate. In addition, this rapid climate change might support the occurrence and timing of the outburst flood event during the Xia Dynasty and might have led to the fall of the Xia Dynasty.

Plain Language Summary Rapid and drastic climate changes will have serious impacts on the ecological environment and the development of human society. Studies on such climate events enable to better understand the relationship between climate change and human civilization, and provide valuable materials for predicting future climate trends. There was an extremely cold event during the period of ∼3,800–3,500 years BP (before present year 1950) in the Middle Bronze Age in North Atlantic and Europe region, which had a serious impact on European civilization. We carry out high-resolution paleoclimate reconstructions during this period by using geochemical tracers in fossil corals from the South China Sea. The results indicate that the South China Sea and even the entire Western Pacific have experienced a rapid cooling and wetting event during the period of ∼3,800–3,500 years BP and the extremely cold event during the Middle Bronze Age was global scale. In addition, the consistency between the coral records and the stalagmite records from the inner land of China suggest that a rapid cooling and drying event during the Middle Bronze Age led to the collapse of the Xia Dynasty and Emperor Yu's success in taming floods was attributed to this event.

1. Introduction

The Holocene is generally considered to be a relatively warm and stable period (Dansgaard et al., 1989; Jouzel et al., 2007) that provided suitable climatic conditions for the development of human society. However, a growing number of studies have found that some rapid climate change events lasting for tens, hundreds, or thousands of years occasionally occurred and led to the collapse of some ancient civilizations (Cullen et al., 2000; Guo et al., 2018; Mayewski et al., 2004; Saraswat et al., 2016; Staubwasser et al., 2003; Wanner et al., 2011; Weiss et al., 1993). Detailed research on these rapid climate changes is helpful to understand their impact on the development of past civilizations, and can provide valuable materials for predicting future climate trends.

The Bronze Age is one of the most important stages in the history of human civilization development, during which the use of bronze tools marked the first time humans started to work with metal and a significant improvement in social productivity occurred (Earle, 2002). Nevertheless, the Middle Bronze Age Cold Epoch (MBACE) was an unusually cold interval in the North Atlantic and European regions that lasted for approximately 300 years, from ~3,800 years BP (before present year 1950) to ~3,500 years BP (Cardoso et al., 2013; Demeny et al., 2019; Gutiérrez Elorza & Sesé Martínez, 2001; Kobashi et al., 2011; Siklósy et al., 2007; Siklósy et al., 2009; Vollweiler et al., 2006). The occurrence of this cold event had a serious impact on the development of human society, and the decline of cities in some parts of Europe has been found to be related to it (e.g., Cretan cities, Siklósy et al., 2007). Meanwhile, the MBACE was in the climate transition stage from the Holocene thermal maximum to the colder late Holocene (~3,000–4,000 years BP) (Edvardsson, 2016; Morley et al., 2014; Wanner et al., 2008), and the rapid climate transitions during the mid-to-late Holocene should be studied intensively because of the very complex mechanisms that occurred, including solar activity fluctuation, volcanic eruption, ocean-atmosphere interaction, and thermohaline circulation (Wanner et al., 2008). However, due to the lack of high-resolution climate records and the short duration of ~300 years of the MBACE, this cooling event has seldom been reported in other places in the world (K. B. Yu et al., 2016), and its details have yet to be explored. Considering the effect of the Atlantic Ocean on global climate systems (e.g., Delworth & Zeng, 2016; Delworth et al., 2016; Han et al., 2019; Y Wang et al., 2005; L Zhang et al., 2017), as well as the effect of rapid climate changes on the evolution of human civilization, it is essential to carry out more high-resolution climate reconstruction studies on other regions during the MBACE.

Geochemical compositions in reef corals are excellent proxies for reconstructing high-resolution past climate records in tropical oceans (Felis & Pätzold, 2003; Lough, 2010), which are widely used for studying the seasonal to millennial scales of climate change over the Pacific region during the Holocene (Cobb et al., 2003; Deng et al., 2017; Deng et al., 2019; Gagan et al., 1998; Gagan et al., 2000; Han et al., 2019). The South China Sea (SCS) is the largest marginal sea in the western tropical Pacific, and coral reefs are widely distributed there (K Yu, 2012). Furthermore, the climate in the SCS is strongly controlled by the East Asian Monsoon (B Wang, 2006), which is linked to the North Atlantic climate (Han et al., 2019; Y Wang et al., 2005). Therefore, the reef coral in the SCS has high potential to record the MBACE-associated climate event over the Asia-Western Pacific region during the mid-to-late Holocene transition.

In this study, we used Sr/Ca and $\delta^{18}O$ signatures with an annual resolution from four fossil corals, whose growth periods exactly cover the period ~3,500–3,800 years BP, to reconstruct the sea surface temperature (SST) and the surface seawater $\delta^{18}O$ ($\delta^{18}O_{sw}$) in the northern SCS. Synthesizing the reconstructed results and existing paleoclimate data from adjacent land and ocean regions, we analyzed the climate characteristics of the Asia-Pacific regions and discussed the relationship between abrupt climate change and ancient civilizations in China during the MBACE.

2. Materials and Methods

Fossil coral cores were drilled from four *Porites lutea* colonies using an underwater pneumatic drill, with diameters of approximately 1.5–2.5 m, from water depths of approximately 2–4 m on the fringing reefs off the east coast of Hainan Island (Figure 1). Coral samples 14QG7 and 14QG8 were collected from Qingge (14QG7: 19°19′06.37"N, 110°40′49.28"E; 14QG8: 19°19′20.52"N, 110°40′0.05"E) in July 2014. Coral sample 14FJ9 was collected from Fengjiawan (19°23′56.94"N, 110°44′12.24"E), also in July 2014. Coral sample 15WC3 was collected from Wenchang (19°24′18.576"N, 110°45′35.604"E) in May 2015.

After the coral cores were sectioned, X-ray photographed (Figure S1) and ultrasonically cleaned, the four fossil corals were U-Th dated using multicollector inductively coupled plasma mass spectrometers at the Radiogenic Isotope Facility of the University of Queensland. The details of the analytical methods are provided in Zhou et al. (2011). Under the guidance of X-radiographs, near-annual resolution subsamples were consecutively collected from annual bands along the maximum growth axis using a digitally controlled

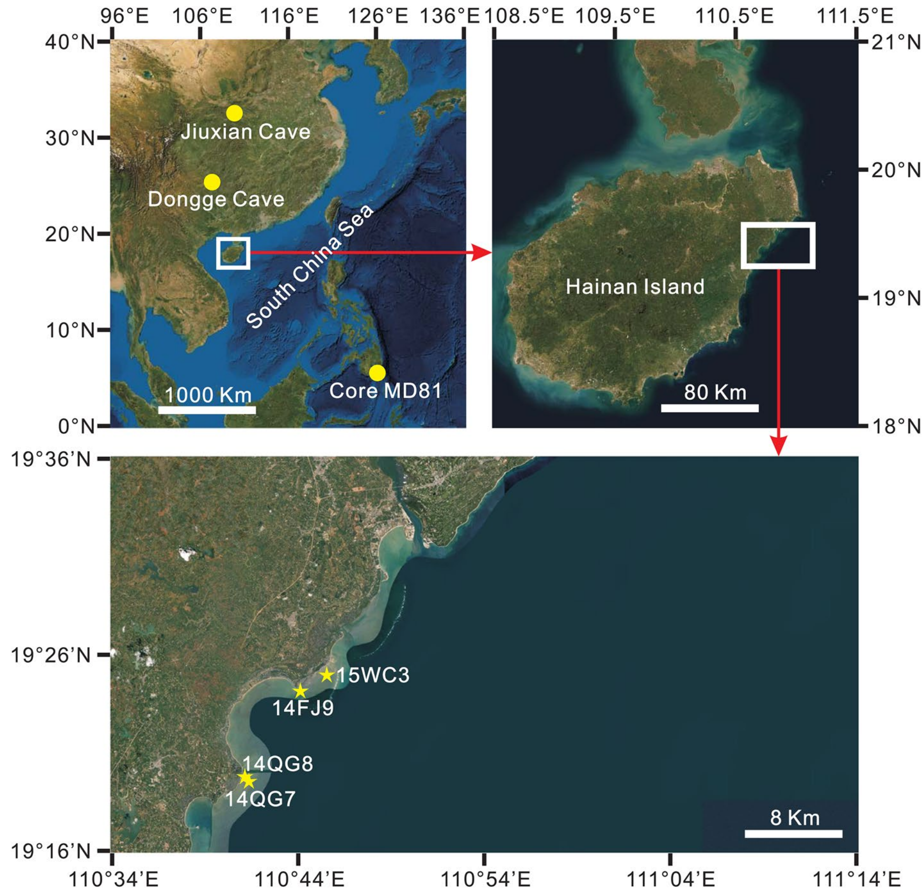

Figure 1. Satellite images of the study region. The yellow stars in the lower panel indicate the coral sampling locations. The yellow solid circles indicate the study sites in the Asia-western Pacific region, which are included for comparison.

milling machine. Each high-density and low-density band constitutes an annual couplet, generally representing one year of growth (Knutson et al., 1972). Raman spectral analyses of the four fossil corals showed that the coral skeletons were 100% aragonite (Figure S2).

Measurements of skeletal Sr/Ca and $\delta^{18}O$ were carried out in the State Key Laboratory of Isotope Geochemistry, Guangzhou Institute of Geochemistry, Chinese Academy of Sciences. For the details of geochemical pretreatment and analytical procedures, refer to Deng et al. (2017). The estimation of $\Delta\delta^{18}O$ (the proxy for $\delta^{18}O_{sw}$) used the same method as that reported in Gagan et al. (2000), i.e., subtracting the temperature contribution from the coral $\delta^{18}O$ according to the equation $\Delta\delta^{18}O = d\delta^{18}O/dT \times [T_{\delta 18O} - T_{Sr/Ca}]$. In this equation, $d\delta^{18}O/dT$ is the slope (0.194‰/°C) of the $\delta^{18}O$–SST relationship ($\delta^{18}O$ (‰) = −0.194 × SST (°C)–0.276) obtained using a modern *Porites lutea* coral from the nearby region in the northern SCS (Song et al., 2006), and $T_{\delta 18O}$ and $T_{Sr/Ca}$ are the reconstructed temperatures from the $\delta^{18}O$ values and Sr/Ca ratios, respectively. The Sr/Ca-SST relationship, Sr/Ca (mmol/mol) = −0.084 × SST (°C) + 11.278, was employed from Gagan et al. (2012), which has been corrected for the attenuation effect of skeletal mass accumulation on coral Sr/Ca and agrees with foraminiferal Mg/Ca records and coral Sr/Ca records in the Indo-Pacific region during the last 14,200 years (Gagan et al., 2012).

For comparisons with previously published palaeoclimatic records, annual SST ($\delta^{18}O_{sw}$) anomalies during each climate period were calculated by centering the SST ($\delta^{18}O_{sw}$) records (subtracting the mean of total data during the four periods from each value).

3. Results

The corrected ^{230}Th ages of coral samples 14QG7, 14QG8 and 14FJ9 were 3,582 ± 17, 3,729 ± 12 and 3,823 ± 12 years (before the year of 2015), respectively, and that of 15WC3 was 3960 ± 9 years (before the year of 2016) (Table 1). The ages of these fossil corals were converted into BP ages, and their growth intervals were ∼3,518–3,711 years BP, ∼3,665–3,757 years BP, ∼3,759–3,847 years BP, and ∼3,895–3,979 years BP, respectively.

The Sr/Ca ratios varied largely from 8.877 mmol/mol to 9.466 mmol/mol during the four periods, with averages of 9.232 mmol/mol, 9.292 mmol/mol, 9.045 mmol/mol, and 9.162 mmol/mol during the periods of ∼3,518–3,711 years BP, ∼3,665–3,757 years BP, ∼3,759–3,847 years BP, and ∼3,895–3,979 years BP, respectively (Figure 2a). Unlike the large variation amplitudes in the Sr/Ca records, the δ^{18}O values remained relatively stable during the four periods, with averages of −5.55‰, −5.65‰, and −5.57‰ for the intervals of ∼3,518–3,711 years BP, ∼3,665–3,757 years BP, and ∼3,759–3,847 years BP, respectively, but a higher level of −5.41‰ occurred during the period of ∼3,895–3,979 years BP (Figure 2b).

According to the variation characteristics in the Sr/Ca records, the SST during the period of ∼3,500–4,000 years BP was not stable and fluctuated rapidly (Figure 2c). The average SST during the period of ∼3,895–3,979 years BP was approximately 25.2 °C and increased to 26.6 °C during the period of ∼3,759–3,847 years BP. Then, the average SST began to decline rapidly to 23.6 °C during the period of ∼3,665–3,757 years BP and then slowly rose to 24.4 °C during the period of ∼3,518–3,711 years BP.

Similar to the SST situation, the variation in $\delta^{18}O_{sw}$ during the study period was also drastic (Figure 2d). The averages of $\delta^{18}O_{sw}$ during the periods of ∼3,895–3,979 years BP and ∼3,759–3,847 years BP were −0.26‰ and −0.15‰, respectively. The average of $\delta^{18}O_{sw}$ also decreased rapidly from −0.15‰ during the period of ∼3,759–3,847 years BP to −0.80‰ during the period of ∼3,665–3,757 years BP and then gradually increased to −0.55‰ during the period of ∼3,518–3,711 years BP.

There was an overlapping period of ∼3,665–3,711 years BP during the ∼3,518–3,711 years BP and ∼3,665–3,757 years BP periods (Figure 2). The averages of Sr/Ca, δ^{18}O, Sr/Ca-SST, and $\delta^{18}O_{sw}$ of this overlapping time window were 9.275 mmol/mol versus 9.284 mmol/mol, −5.58‰ versus -5.61‰, 23.8 versus 23.7 °C, and −0.69‰ versus −0.74‰, respectively, during the periods of ∼3,518–3,711 years BP and ∼3,665–3,757 years BP. The Sr/Ca-SST and the $\delta^{18}O_{sw}$ in the overlapping time window were averaged to generate the final time series for the discussion.

4. Discussion

4.1. The Reliability of the Coral Records

Despite the advantage of the high resolution of coral records, their disadvantage is that they are relatively shorter-lived, usually lasting only several hundred years, than other natural climate archives (Felis & Pätzold, 2003). Splicing multiple coral records together to generate a longer record is a good way to overcome this barrier to study climate changes on longer time scales (Abram et al., 2009; Cobb et al., 2003; Deng et al., 2019). The precision of U-Th dating for Holocene coral carbonates can be as high as ∼1 year under the current analytical technology (X Wang et al., 2018; Yan et al., 2019). The precision in the study is from 9 to 12 (±2σ) years, which is still better than the best precision of 18–20 (±1σ) years of Holocene samples by the ^{14}C dating method (Bush et al., 2013; Nakamura et al., 2016). Therefore, rapid climate changes that are sufficiently fast (a few hundred years or shorter) from the point of view of human civilization (Mayewski et al., 2004) can be well resolved and constrained by coral records. Consequently, the coral records in this study are suitable to explore the climate characteristics in the northern SCS during the MBACE.

The largest SST variation amplitude (maximum minus minimum) from ∼3,759 to 3,847 years BP to ∼3,665 to 3,757 years BP recorded by coral records is ∼7°C, and the average SST difference is ∼3°C during these two periods. The reasonability of such a large change during the ∼200 years should be evaluated before it is used to discuss climate change.

Although the mineral composition of the fossil coral skeletons used in this study is 100% aragonite (Figure S2), Raman spectroscopy could not detect the presence of secondary aragonite cements. The secondary

10.1029/2020JC016964

Table 1
MC-ICP-MS U-Th Dating Results for the Fossil Corals

Sample name	U (ppm)	±2σ	^{232}Th (ppb)	±2σ	^{230}Th/^{232}Th	±2σ	^{230}Th/^{238}u	±2σ	^{234}U/^{238}U	±2σ	Uncorrected ^{230}Th age (yr)	±2σ	Corrected ^{230}Th age (yr)	±2σ	Initial ^{234}U/^{238}U	±2σ
14QG7	3.3469	0.0017	3.715	0.004	101.92	0.25	0.03728	0.00008	1.1455	0.0013	3611	9.0	3582	17	1.1470	0.0013
14QG8	3.5672	0.0010	1.699	0.002	245.64	0.66	0.03862	0.00009	1.1458	0.0009	3741	10.0	3729	12	1.1473	0.0010
14FJ9	3.1158	0.0015	1.163	0.001	321.00	0.95	0.03949	0.00011	1.1444	0.0010	3832	11.0	3823	12	1.1460	0.0011
15WC3	3.0902	0.0008	0.617	0.001	621.30	1.40	0.04090	0.00008	1.1445	0.0009	3.966	9.0	3960	9	1.1461	0.0009

Note. The ratios are activity ratios calculated from atomic ratios using decay constants of Cheng et al. (2000). All values have been corrected for laboratory procedural blanks. Uncorrected ^{230}Th age (yr) was calculated using the Isoplot/EX 3.0 program (Ludwig, 2012), where yr denotes year.

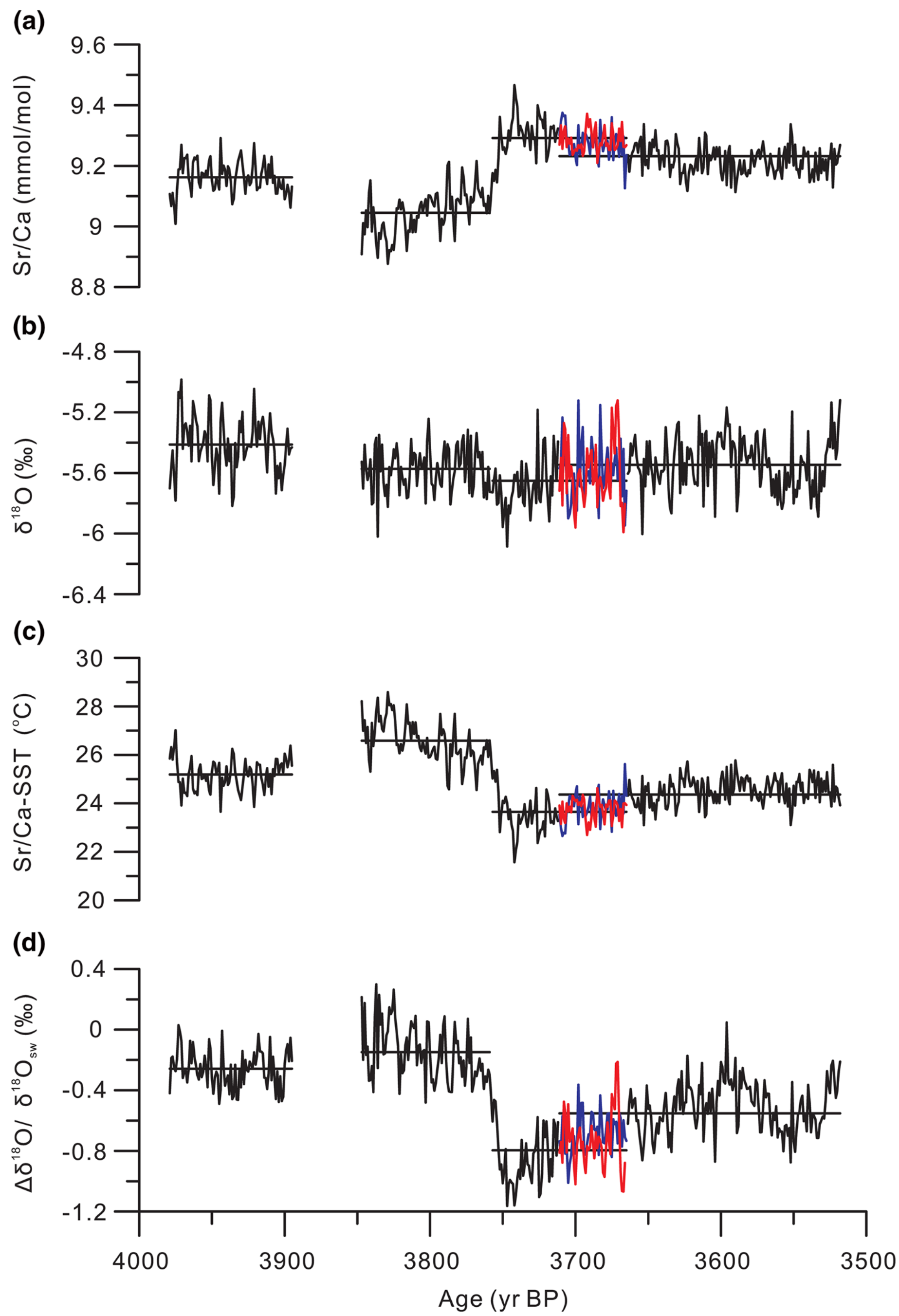

Figure 2. Time series of (a) coral Sr/Ca, (b) coral $\delta^{18}O$, (c) SST reconstructed from coral Sr/Ca, and (d) $\delta^{18}O_{sw}$ reconstructed from paired coral Sr/Ca and $\delta^{18}O$. The records in the two time windows overlap each other during the periods of ~3,518–3,711 years BP and ~3,665–3,757 years BP, which are highlighted in blue and red, respectively. The horizontal lines indicate the averages of different geochemical variables and records for different periods. SST, sea surface temperature.

aragonite cements contain significantly more Sr than the original aragonite skeleton, and only ~2% secondary aragonite cement contamination can cause a significant deviation of −0.4 to −0.9°C in the estimation of Sr/Ca-SST (Allison et al., 2007). Therefore, for those points where the Sr/Ca ratio is particularly high, further petrological examinations were carried out, but no secondary aragonite cement was found (Figures S3 and S4). Thus, it can be determined that the samples used in this study are all primary coral aragonite and have not undergone any post-depositional diagenesis.

Considering that all the coral Sr/Ca ratios were analyzed and calibrated against the same coral standard reference material (i.e., JCp-1, Hathorne et al., 2013; Okai et al., 2002) and converted to temperature records by the same Sr/Ca–SST relationship (Gagan et al., 2012). The long-term analysis of the JCp-1 as a quality control standard yielded a Sr/Ca ratio of 8.829 mmol/mol with the reproducibility of 0.16% (relative standard deviation), which is consistent with the reference value of 8.838 mmol/mol within the error range (Hathorne et al., 2013). Therefore, the errors due to the analytical and calculation methods (0.16%) may not induce a temperature uncertainty as large as 3°C. As extracted from biological carbonates, coral Sr/Ca is inevitably subject to intercolonial differences (Alpert et al., 2016; Pfeiffer et al., 2009; Zinke et al., 2016), which may compromise the reconstructed SST records. Previous studies on living corals in the northern SCS have shown that such an effect significantly affects Sr/Ca SST estimates by 1.7°C (Deng et al., 2019; Y Liu et al., 2013), comparable to another assessment of fossil corals, which suggests an ~1.6°C bias in SST reconstruction (Abram et al., 2009). Additionally, lower temperatures (e.g., a winter temperature of ~18°C) would decrease calcification rates and lead to a higher distribution coefficient ($D = \mathrm{Sr/Ca_{coral}/Sr/Ca_{seawater}}$) and, consequently, a high Sr/Ca ratio in the coral skeleton, which will amplify the SST change by ~2-fold (McCulloch et al., 1994). Assuming this effect is applicable for the coral records during the coldest stage in this study and the variation amplitude of ~7°C has been amplified by ~2-fold, the original SST variation amplitude of ~3.5°C is still significantly larger than the temperature error induced by inter-colony differences (~1.6°C). Therefore, the large SST variation amplitude in this study should not result from the uncertainties induced by analytical and vital effects. Based on a coupled ocean-atmosphere model, rapid climate transitions can result in a drop in average SST in the north Atlantic by up to 5°C within less than 10 years (Rahmstorf, 1994). Considering the above scenarios, the large variation amplitudes and the average difference in SST records within ~200 years during the MBACE reconstructed from coral Sr/Ca should be reasonable. However, due to the lack of other high resolution records for confirmation, the largest SST variation amplitude of ~7°C still should be cautious.

Likewise, the largest $\delta^{18}O_{sw}$ variation amplitude (~1.40‰) also occurred in the transition from ~3,759–3,847 years BP to ~3,665–3,757 years BP, and the average $\delta^{18}O_{sw}$ difference was approximately 0.65‰ during these two periods. If the uncertainty of 0.12–0.17‰ assessed by the inter-colony reproducibility of $\delta^{18}O_{sw}$ based on the central tropical Pacific corals is employed here (Nurhati et al., 2011), then the $\delta^{18}O_{sw}$ variations are significant and may reflect seawater chemistry changes in the northern SCS during this rapid climate transition.

If the dating errors are not considered, the two time windows of ~3,518–3,711 years BP and ~3,665–3,757 years BP exactly overlap each other. The averages of SST and $\delta^{18}O_{sw}$ of the overlapping window (23.8°C and −0.69‰ during ~3,518–3,711 years BP, 23.7°C and −0.74‰ during ~3,665–3,757 years BP) are identical in terms of analytical precision, which indicates that the reconstructed records from fossil corals are reliable for studying the climate transition during the MBACE.

4.2. Comparisons with Other Records

4.2.1. SST

Generally, the average SST (~26.6°C) during the period of ~3,759–3,847 years BP is the same as the estimate for the current warm period in the northern SCS (Deng et al., 2017), indicating a relatively warm period during this time frame. However, after this period, a rapid cooling event had occurred since ~3,850 years BP and lasted until ~3,750 years BP, after which the SST displayed a relatively stable and gradually increasing trend (Figure 2c). There is no other high-resolution SST record with similar chronological uncertainty as ours in the study site, so we compared our results with two relatively low-resolution reconstructions from the nearby region: the long-chain alkenone unsaturation index $\left(U_{37}^{K'}\right)$ from the Pearl River Estuary in the northern SCS (Kong et al., 2014) and the foraminiferal Mg/Ca ratio from Indonesia in the western Pacific (Stott et al., 2004). The comparisons show that the reconstructed SSTs exhibit similar variation patterns, which provides evidence to support the rapid cooling event recorded in our coral records during the MBACE (Figures 3a and b). In detail, the $U_{37}^{K'}$-SST record from the northern SCS shows a decrease of ~1.0°C from ~3,821 years BP to ~3,773 years BP. This decrease in amplitude is much lower than that of ~3.0°C recorded by coral Sr/Ca, but it is still larger than the adjacent variation amplitudes in this time series, indicating an

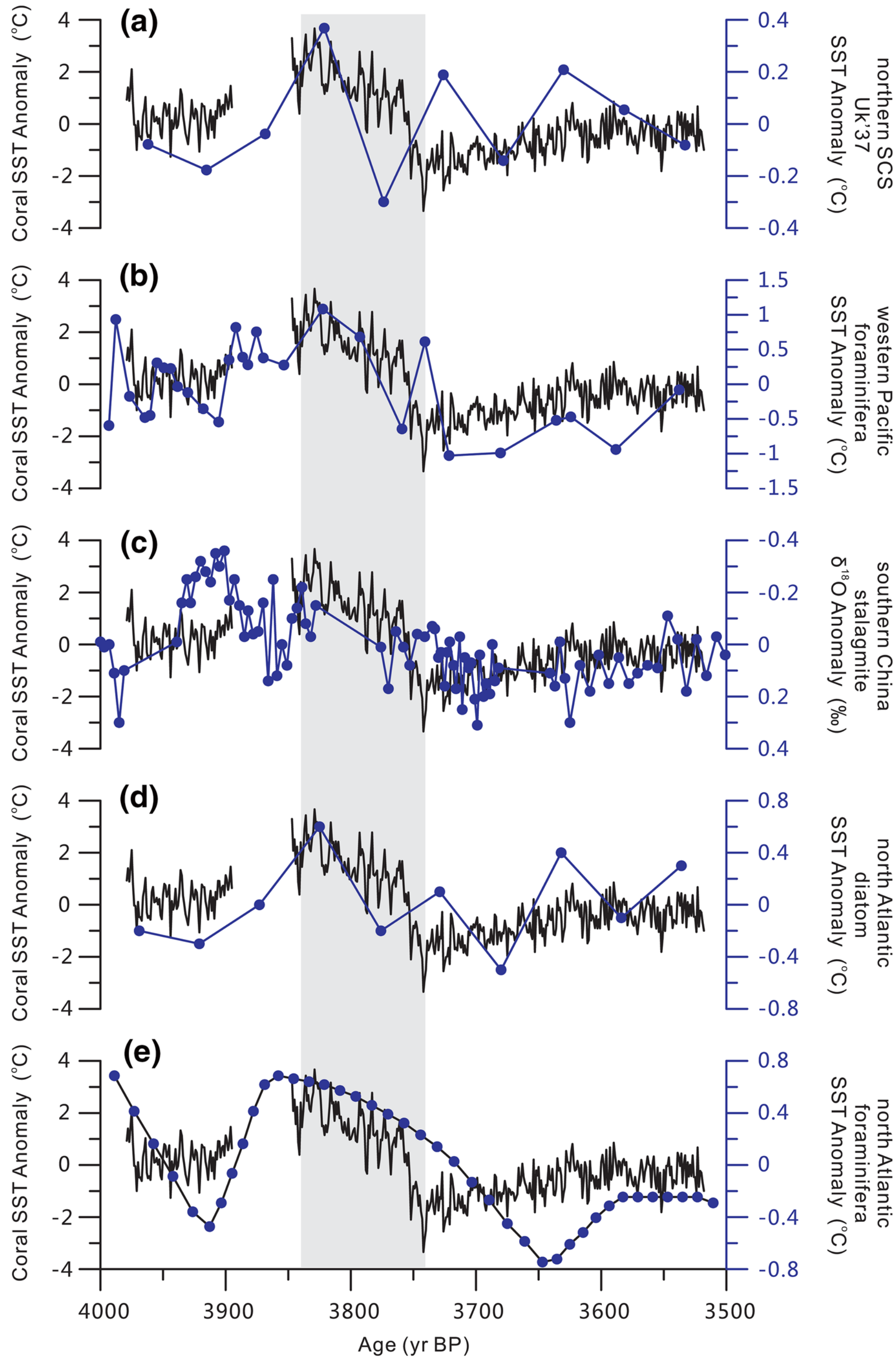

Figure 3. Comparison of SST records based on coral Sr/Ca time series from the northern SCS with the (a) long-chain alkenone unsaturation index SST records from the Pearl River Estuary in the northern SCS (Kong et al., 2014), (b) SST records reconstructed from foraminiferal Mg/Ca profiles in sediment core MD81 from Indonesia in the western Pacific (Stott et al., 2004), (c) stalagmite $\delta^{18}O$ records from Dongge Cave in southern China (Y Wang et al., 2005), (d) diatom transfer function-based SST records from Iceland in the North Atlantic (Jiang et al., 2015), and (e) planktonic foraminiferal analogue function-based SST records from the Irminger Sea in the North Atlantic (Mayewski et al., 2004). The black lines are coral records, and the blue lines with solid circles indicate other records. The gray vertical bar denotes the rapid cooling during the period of ~3,750–3,850 years BP. Note that stalagmite $\delta^{18}O$ record is plotted on an inverted scale on the y axis to allow the comparison between the coral SST and the Asian summer monsoon strength. SST, sea surface temperature.

abrupt temperature change. The foraminiferal Mg/Ca-SST record from the western tropical Pacific Ocean presents a cooling amplitude of ~2.1°C from ~3,822 years BP to ~3,721 years BP. Although this amplitude is still lower than the ~3.0°C cooling amplitude in our study, it should be reasonable because the SST in tropical oceans is more stable than that in high latitude sea areas.

A high-resolution (~5 years) stalagmite $\delta^{18}O$ record from Dongge Cave in southern China was also taken to compare with the coral records (Figure 3c), which represents the evolution history of the Asian summer monsoon strength during the Holocene (a more negative $\delta^{18}O$ value indicates a stronger summer monsoon; Y Wang et al., 2005). The strength of the Asian summer monsoon decreased rapidly from ~3,839 years BP to ~3,699 years BP with the increase in stalagmite $\delta^{18}O$ from −8.05‰ to −7.52‰. Considering that the stronger Asian summer monsoon brings warmer Indo-Pacific ocean surface water to the SCS, increasing SST there, and vice versa (Steinke et al., 2006), this characteristic in the stalagmite $\delta^{18}O$ record agrees with our coral record.

Considering that the MBACE was reported in the North Atlantic in previous studies, some records from the North Atlantic and adjacent regions were also incorporated here for comparative study. An ~50-years resolution diatom transfer function-based SST record from Iceland shows a SST decline of ~1.1°C from ~3,825 years BP to ~3,680 years BP (Figure 3d) (Jiang et al., 2015). Another North Atlantic high-resolution (~12 years) planktonic foraminiferal analogue function-based SST record from the Irminger Sea in the North Atlantic suggests a decrease of ~1.5°C during the period of ~3,850 years BP to ~3,650 years BP (Figure 3e) (Mayewski et al., 2004).

Although spliced from four fossil corals, the SST record in our study is still a little bit short. In addition, the chronological uncertainty of the paleoclimatic records used for comparative study may compromise the identification of this rapid cooling event. Therefore, it is essential to place this cooling event into a longer climatic context for further examination. It can be found that the cooling event identified by our coral record is also evident and comparable to other rapid changes in above mentioned records even in the context of ~5,000–3,000 years BP (Figure S5). Synthesizing above analyses, it is reasonable to infer that there was a rapid cooling event both in the North Atlantic and the western Pacific, and the variation amplitude was much larger in the coastal area of the marginal sea of the western Pacific during the MBACE.

Previous studies have suggested that the frequent volcanic activities during this period might be responsible for the cold conditions during the MBACE (Siklósy et al., 2007; Siklósy et al., 2009) because some major volcanic eruptions, such as Avellino (Sevink et al., 2011) and Thera (Pearson et al., 2018), occurred during the mid-to-late Holocene transition. However, the variation trends of the volcanic forcing index (Kobashi et al., 2017) and these SST records do not match very well ($r = 0.003$, $n = 406$, $p = 0.48$, Pearson correlation analysis) (Figure 4a), and the stronger volcanic activities (corresponding to more negative forcing values) suggested by the volcanic forcing index occurred during the period of ~3,500–3,600 years BP. This time window was obviously later than the beginning of this rapid cooling. Considering the reliability of U-Th absolute dating, it is unlikely that the rapid cooling was triggered by volcanic eruptions. However, it is still possible that volcanic eruptions maintained a relatively cold status until the end of the MBACE. Solar variability is a more plausible forcing for rapid climate changes during the Holocene (Mayewski et al., 2004), but the variation in total solar irradiance (TSI) (Steinhilber et al., 2009) during the study period did not always agree with that of the SST record ($r = 0.14$, $n = 414$, $p < 0.01$, Pearson correlation analysis based on linearly interpolated TSI data) except during the rapid cooling period (~3,727–3,822 years BP) (Figure 4b). Therefore, solar variability was a possible factor in triggering rapid cooling. Some studies have also suggested that the change in the thermohaline circulation was responsible for the rapid cold event lasting several hundred years, such as occurred during the 8.2 ka event (~8,000–8,400 years BP) and during the Little Ice Age (LIA, ~1500–1900 CE) (Broecker, 2000; Keigwin & Boyle, 2000). For this reason, the possibility of the role of the thermohaline circulation, especially the Atlantic Meridional Overturning Circulation (AMOC), on this rapid cooling event should be considered because the AMOC could be one of the primary forcings that caused the 8.2 ka cold event (Cheng et al., 2009).

A recent study suggested that the intensified Asian winter monsoon led to a SST drop of up to ~4°C at the northern coast of the SCS during the periods of LIA and ~2,500–1,200 years BP (Y Zhang et al., 2019). Based on the comparison between the coral record and the Asian winter monsoon intensity index (the magnetic

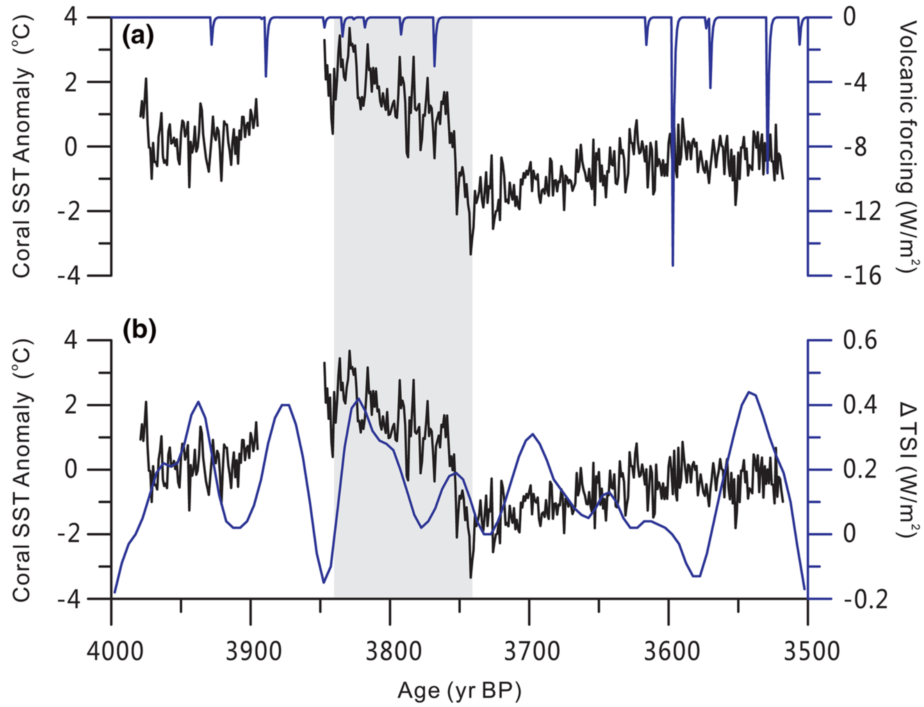

Figure 4. Comparison of SST records based on coral Sr/Ca time series from the northern SCS with the (a) volcanic forcing index generated from the sulphate concentration record of GISP2 (Kobashi et al., 2017) and (b) TSI reconstructed based on the cosmogenic radionuclide ^{10}Be (Steinhilber et al., 2009). The black lines are the coral records, and the blue lines indicate the other records. The gray vertical bar denotes the rapid cooling during the period of ~3,750–3,850 years BP. SST, sea surface temperature; TSI, total solar irradiance.

susceptibility of sediment core from Lake Huguang Maar, Southeast China) (Yancheva et al., 2007), the intensification of winter monsoon only occurred during ~3,850–3,800 years BP and the secular drop in SST was observed throughout the whole cooling period (Figure S6). Therefore, the role of the Asian winter monsoon in this cooling period should not be neglected and need further study.

The study sites are located in the area affected by the summer monsoon-induced upwelling system along the east coast of Hainan Island (Jing et al., 2009), and SST may register the upwelling signal, which has been demonstrated by coral Sr/Ca records from the same area (Y Liu et al., 2013). However, the stalagmite $\delta^{18}O$ record suggested the decrease in summer monsoon during ~3,850–3,750 years BP (Figure 3c). Therefore, it seems not possible that the rapid cooling event might represent a strong upwelling signal by enhanced summer monsoon.

4.2.2. $\delta^{18}O_{sw}$

Similar to the comparative study of the SST record, some nearby records covering the study period were employed to explore the hydrological conditions in the northern SCS during the MBACE. The variation pattern of $\delta^{18}O_{sw}$ is very similar to that in the western tropical Pacific Ocean reconstructed from foraminiferal Mg/Ca and $\delta^{18}O$ in sediment core MD81 (Stott et al., 2004), which suggests that the two study sites experienced a similar hydrological variation during the mid-to-late Holocene climate transition. Both $\delta^{18}O_{sw}$ records show a rapid decline during the period of ~3,850–3,750 years BP (Figure 5a), but their variation amplitudes are different. Similar to the situation in their SST records, the variation amplitude of the average $\delta^{18}O_{sw}$ (~0.95‰) in the northern SCS is almost two times larger than that (~0.57‰) in the western tropical Pacific Ocean (Figure 5a). The variation amplitude of ~0.95‰ during the rapid cooling period is comparable to that of $\delta^{18}O_{sw}$ at the century time scale since ~7000 years BP synthesized by the coral records from the northern SCS (Yan et al., 2019), and corresponds to a decrease of ~3.8 psu in sea surface salinity as estimated from the $\delta^{18}O_{sw}$-salinity relationship (~0.25‰/psu, Ye et al., 2014). However, this decreased amplitude in salinity

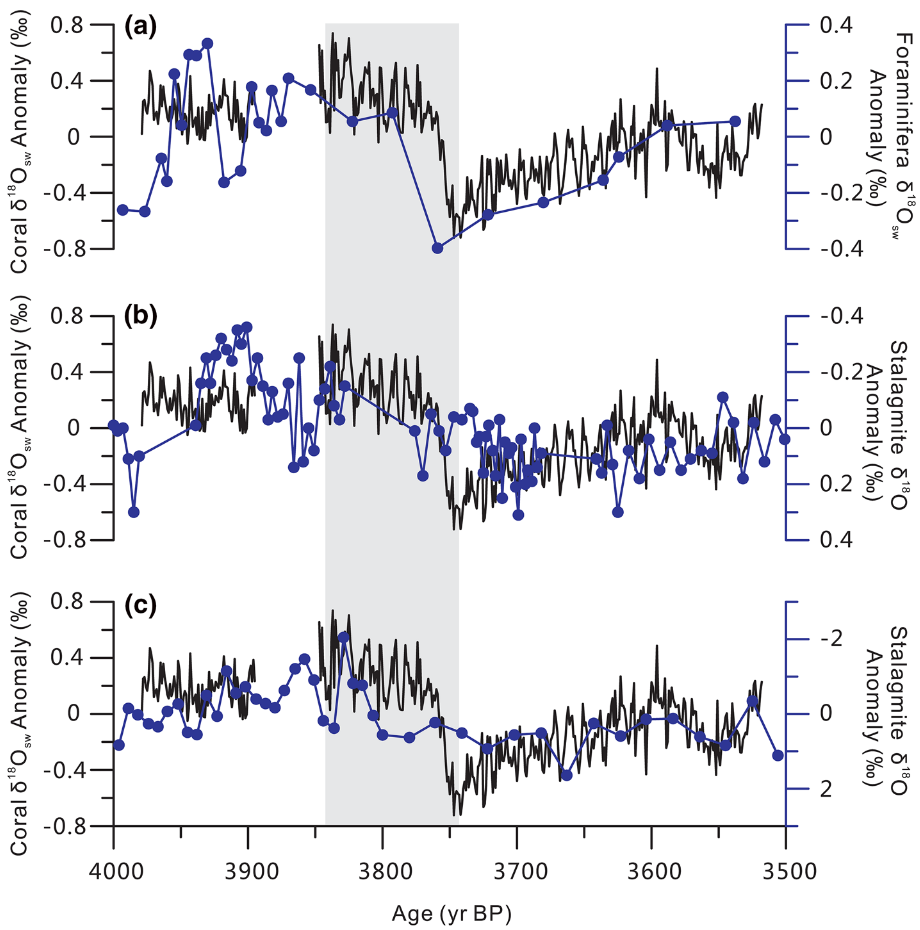

Figure 5. Comparison of $\delta^{18}O_{sw}$ records based on coral Sr/Ca and $\delta^{18}O$ time series from the northern SCS with the (a) $\delta^{18}O_{sw}$ records based on foraminiferal Mg/Ca and $\delta^{18}O$ in sediment core MD81 from Indonesia in the western Pacific (Stott et al., 2004), (b) stalagmite $\delta^{18}O$ records from Dongge Cave in southern China (Y Wang et al., 2005), and (c) stalagmite $\delta^{18}O$ records from Jiuxian Cave in northern China (Cai et al., 2010). The black lines are the coral records, and the blue lines with solid circles indicate the other records. The gray vertical bar denotes the rapid cooling during the period of ~3,750–3,850 years BP. Note that stalagmite $\delta^{18}O$ records are plotted on an inverted scale on the y axis to allow a comparison with coral $\delta^{18}O_{sw}$ records.

is much larger than the annual variation range in modern instrumental record (~1.0 psu, Zeng et al., 2018; Yi et al., 2020), indicating a very different hydrological condition during the rapid cooling period.

In addition to the stalagmite $\delta^{18}O$ record from southern China for the comparative study with SST (Y Wang et al., 2005), another record from Jiuxian Cave in northern China was also included here to strengthen the reliability of the coral records (Cai et al., 2010). These two stalagmite $\delta^{18}O$ records reflected the strength of the Asian summer monsoon and the amount of summer monsoon precipitation (Cai et al., 2010; Y Wang et al., 2005). The coral $\delta^{18}O_{sw}$ record and the two stalagmite $\delta^{18}O$ records have opposite variation trends during the study period, which is most obvious during the period of ~3,850–3,750 years BP (Figures 5b and c). Specifically, the coral $\delta^{18}O_{sw}$ record displayed a rapid decrease during the period of ~3,850–3,750 years BP, but both stalagmite $\delta^{18}O$ records increased rapidly during that period (Figures 5b and 5c). The opposite variation trends resulted from the fact that the position of the rain belt is northward when the Asian summer monsoon is strong and southward when it is weak (Shi & Zhu, 1996). Therefore, more water vapor was transported to the inner land of China, and the SCS was relatively dry when the Asian summer monsoon was stronger, which led to more negative stalagmite $\delta^{18}O$ values and more positive coral $\delta^{18}O_{sw}$ values. This scenario has also been indicated by other coral records from the northern SCS during the mid-Holocene with enhanced Asian summer monsoon, which can be demonstrated by an atmosphere-ocean coupled general circulation model (Yokoyama et al., 2011). In details, they observed northward shift of inter tropical convergent zone by the enhanced Asian summer monsoon in the model experiments that produced increased precipitation on the Asian continent, and therefore the increase in salinity was due to less precipitation in the SCS and increased continental precipitation inland of Asia (Yokoyama et al., 2011). The opposite situations occurred when the Asian summer monsoon became weaker. However, Chinese stalagmite $\delta^{18}O$ record does not necessarily represent the amount of summer monsoon precipitation and its interpretation is time scale dependent (Hu et al., 2019; X Liu et al., 2020). The stalagmite $\delta^{18}O$ is possibly also associated with the change in moisture source controlled by the intensity of monsoonal circulation at interannual scales, and increased moisture delivery from remote source regions will lead to more negative precipitation $\delta^{18}O$ over China when the Asian summer monsoon is stronger (Hu et al., 2019). Therefore, the changes in stalagmite $\delta^{18}O$ records still can be linked to those in the intensity of the Asian summer monsoon. Considering that these records from different proxies can cross-verify the reconstruction reliability when demonstrating ocean and land surface hydrological conditions during the period of ∼3,850–3,750 years BP in this study, the variations in $\delta^{18}O_{sw}$ during the study period were mainly dominated by the Asian summer monsoon, but the changes in the Holocene Asian summer monsoon were linked with solar changes and the North Atlantic climate (Y Wang et al., 2005). Accordingly, the MBACE originally found in and around North Atlantic regions might also have occurred in the western Pacific and adjacent regions since there is broad agreement among the coral, foraminiferal, and stalagmite records. This event has not previously been a concern in the paleoclimate community because of the issues of time resolution and dating errors.

4.3. Possible Effect on the Alternation in Chinese Dynasties

The most prominent change during the whole study period is the rapid climate change from ∼3,850 years BP to ∼3,750 years BP, during which the climate over the northern SCS became cold and wet over ∼100 years from previously warm and dry conditions. The Asian summer monsoon declined rapidly, and the inner land of China became cold and dry abruptly. A previous study has indicated that the climate conditions associated with the strength of the Asian monsoon dominated the rise and fall of Chinese dynasties during the past 1,810 years (P Zhang et al., 2008). Therefore, the possible effect of the rapid climate change recorded by the coral records on the alternation of Chinese dynasties was explored here. The Xia Dynasty (2207–1766 BCE) (Michaud, 1997) ended at ∼3716 years BP, which was almost during the rapid climate change period of ∼3,850–3,750 years BP suggested in this study. Consequently, there is a possibility that the collapse of the Xia Dynasty was linked with this rapid cooling and drying event during the MBACE. According to Guoyu, a Bamboo Slats Annal by Chinese historian Qiuming Zuo (556–451 BCE), the Xia Dynasty collapsed when the Yi and Luo Rivers dried up, suggesting a dry climate at the end of the Xia Dynasty. In addition, there was an outburst flood on the Yellow River at ∼3,870 years BP during the beginning of the Xia Dynasty (Wu et al., 2016). This flood time window agrees with that of the most positive coral $\delta^{18}O_{sw}$ values and the most negative stalagmite $\delta^{18}O$ values associated with the stronger Asian summer monsoon, indicating dry conditions in the SCS and wet conditions in inland China (Figure 5). Thus, this study may support the occurrence and timing of the outburst flood event during the Xia Dynasty in Wu et al. (2016). Meanwhile, the rapid drying process indicated by stalagmite records corresponding to the rapid wetting process indicated by coral records may provide evidence for the interesting conjecture that Emperor Yu's success in taming floods was attributed to cooling and drying rather than to his innovations in dredging, dikes, and divisions (W. Wu & Ge, 2005).

5. Conclusions

In this study, the climate conditions with an annual resolution in the northern SCS during the period of ∼3,500–4,000 years BP, the mid-to-late Holocene transition, were determined by splicing several coral geochemical records together. The results indicate that the northern SCS experienced a rapid cooling and wetting process lasting ∼100 years beginning in ∼3,800 years BP and that these cold and wet conditions remained relatively stable from ∼3,750 years BP to ∼3,500 years BP. The rapid climate change process was imprinted in coral, foraminifera and stalagmite records from China and the western Pacific. Combined with several records from the North Atlantic, this cold event is similar to the MBACE, may represent a global-scale climate change, and may be linked with the changes in solar irradiance and the North Atlantic climate. The results may also support the occurrence and timing of the outburst flood event during the Xia

Dynasty and indicate that the fall of the Xia Dynasty might have resulted from this rapid cooling and drying climate in northern China during the MBACE.

Data Availability Statement

The data for this study are available in Zenodo repository (https://doi.org/10.5281/zenodo.4248194).

Acknowledgments
The authors would like to thank the editor Peter G. Brewer and two anonymous reviewers for their helpful comments and constructive suggestions. This work was supported by the Strategic Priority Research Program of Chinese Academy of Sciences (XDB40010300), the National Key Research and Development Program of China (2016YFA0601204), the Key Special Project for Introduced Talents Team of Southern Marine Science and Engineering Guangdong Laboratory (Guangzhou) (GML2019ZD0308), the National Natural Science Foundation of China (41673115, 41722301 and 41803017), Guangdong Basic and Applied Basic Research Foundation (2019A1515010892) and the Chinese Academy of Science (2018g0019). This is contribution No. IS-2952 from GIGCAS.

References

Abram, N. J., McGregor, H. V., Gagan, M. K., Hantoro, W. S., & Suwargadi, B. W. (2009). Oscillations in the southern extent of the Indo-Pacific warm pool during the mid-Holocene. *Quaternary Science Reviews*, *28*(25), 2794–2803. https://doi.org/10.1016/j.quascirev.2009.07.006

Allison, N., Finch, A. A., Webster, J. M., & Clague, D. A. (2007). Palaeoenvironmental records from fossil corals: The effects of submarine diagenesis on temperature and climate estimates. *Geochimica et Cosmochimica Acta*, *71*(19), 4693–4703. https://doi.org/10.1016/j.gca.2007.07.026

Alpert, A. E., Cohen, A. L., Oppo, D. W., DeCarlo, T. M., Gove, J. M., & Young, C. W. (2016). Comparison of equatorial Pacific sea surface temperature variability and trends with Sr/Ca records from multiple corals. *Paleoceanography*, *31*(2), 252–265. https://doi.org/10.1002/2015PA002897

Broecker, W. S. (2000). Was a change in thermohaline circulation responsible for the Little Ice Age? *Proceedings of the National Academy of Sciences*, *97*(4), 1339–1342. https://doi.org/10.1073/pnas.97.4.1339

Bush, S. L., Santos, G. M., Xu, X., Southon, J. R., Thiagarajan, N., Hines, S. K., & Adkins, J. F. (2013). Simple, rapid, and cost effective: A screening method for ^{14}C analysis of small carbonate samples. *Radiocarbon*, *55*(2), 631–640. https://doi.org/10.1017/s0033822200057787

Cai, Y., Tan, L., Cheng, H., An, Z., Edwards, R. L., Kelly, M. J., et al (2010). The variation of summer monsoon precipitation in central China since the last deglaciation. *Earth and Planetary Science Letters*, *291*(1), 21–31. https://doi.org/10.1016/j.epsl.2009.12.039

Cardoso, S., Valverde, L., Alfonso-Sanchez, M. A., Palencia-Madrid, L., Elcoroaristizabal, X., Algorta, J., et al. (2013). The expanded mtDNA phylogeny of the Franco-Cantabrian Region upholds the Pre-Neolithic genetic substrate of Basques. *PLoS ONE*, *8*(7), e67835. https://doi.org/10.1371/journal.pone.0067835

Cheng, H., Edwards, R. L., Hoff, J., Gallup, C. D., Richards, D. A., & Asmerom, Y. (2000). The half-lives of uranium-234 and thorium-230. *Chemical Geology*, *169*(1-2), 17–33. https://doi.org/10.1016/s0009-2541(99)00157-6

Cheng, H., Fleitmann, D., Edwards, R. L., Wang, X., Cruz, F. W., Auler, A. S., et al. (2009). Timing and structure of the 8.2 kyr B.P. event inferred from δ18O records of stalagmites from China, Oman, and Brazil. *Geology*, *37*(11), 1007–1010. https://doi.org/10.1130/g30126a.1

Chen, X., Liu, Z., Wang, H., Xu, D., & Wang, L. (2019). Significant salinity increase in subsurface waters of the South China Sea during 2016–2017. *Acta Oceanologica Sinica*, *38*(11), 51–61. https://doi.org/10.1007/s13131-019-1498-z

Cobb, K. M., Charles, C. D., Cheng, H., & Edwards, R. L. (2003). El Niño/Southern Oscillation and tropical Pacific climate during the last millennium. *Nature*, *424*(6946), 271–276. https://doi.org/10.1038/nature01779

Cullen, deMenocal, H. M.P. B., Hemming, S., Hemming, G., Brown, F. H., Guilderson, T., & Sirocko, F. (2000). Climate change and the collapse of the Akkadian empire: Evidence from the deep sea. *Geology*, *28*(4), 379–382. https://doi.org/10.1130/0091-7613(2000)28<379:ccatco>2.0.co;2

Dansgaard, W., White, J. W. C., & Johnsen, S. J. (1989). The abrupt termination of the Younger Dryas climate event. *Nature*, *339*(6225), 532–534. https://doi.org/10.1038/339532a0

Delworth, T. L., & Zeng, F. (2016). The impact of the North Atlantic Oscillation on climate through its influence on the Atlantic meridional overturning circulation. *Journal of Climate*, *29*(3), 941–962. https://doi.org/10.1175/jcli-d-15-0396.1

Delworth, T. L., Zeng, F., Vecchi, G. A., Yang, X., Zhang, L., & Zhang, R. (2016). The North Atlantic Oscillation as a driver of rapid climate change in the Northern Hemisphere. *Nature Geoscience*, *9*(7), 509–512. https://doi.org/10.1038/ngeo2738

Demeny, A., Kern, Z., Czuppon, G., Nemeth, A., Scholl-Barna, G., Siklosy, Z., et al (2019). Middle Bronze Age humidity and temperature variations, and societal changes in East-Central Europe. *Quaternary International*, *504*, 80–95. https://doi.org/10.1016/j.quaint.2017.11.023

Deng, W., Liu, X., Chen, X., Wei, G., Zeng, T., Xie, L., & Zhao, J.-x. (2017). A comparison of the climates of the medieval climate anomaly, Little Ice Age, and current warm period reconstructed using coral records from the northern South China Sea. *Journal of Geophysical Research: Oceans*, *122*(1), 264–275. https://doi.org/10.1002/2016JC012458

Deng, W., Wei, G., Zhao, J.-x., & Zeng, T. (2019). Anthropogenic effects on tropical oceanic climate change and variability: An insight from the South China Sea over the past 2000 years. *Quaternary Science Reviews*, *206*, 56–64. https://doi.org/10.1016/j.quascirev.2018.12.027

Earle, T. K. (2002). *Bronze age economics: The beginnings of political economies.*, Boulder, Colorado: Westview Press.

Edvardsson, J. (2016). Mid- to Late Holocene climate transition and moisture dynamics inferred from South Swedish tree-ring data. *Journal of Quaternary Science*, *31*(3), 256–264. https://doi.org/10.1002/jqs.2863

Felis, T., & Pätzold, J. (2003). Climate records from corals. In G. Wefer, F. Lamy, & F. Mantoura (Eds.), *Marine science frontiers for Europe* (pp. 11–27). Berlin, Heidelberg, New York, Tokyo: Springer-Verlag.

Gagan, M. K., Ayliffe, L. K., Beck, J. W., Cole, J. E., Druffel, E. R. M., Dunbar, R. B., & Schrag, D. P. (2000). New views of tropical paleoclimates from corals. *Quaternary Science Reviews: Space Physics*, *19*(1), 45–64. https://doi.org/10.1016/S0277-3791(99)00054-2

Gagan, M. K., Ayliffe, L. K., Hopley, D., Cali, J. A., Mortimer, G. E., Chappell, J., et al (1998). Temperature and surface-ocean water balance of the mid-Holocene tropical Western Pacific. *Science*, *279*(5353), 1014–1018. https://doi.org/10.1126/science.279.5353.1014

Gagan, M. K., Dunbar, G. B., & Suzuki, A. (2012). The effect of skeletal mass accumulation in Porites on coral Sr/Ca and $\delta^{18}O$ paleothermometry. *Paleoceanography*, *27*(1). https://doi.org/10.1029/2011PA002215

Guo, L., Xiong, S., Ding, Z., Jin, G., Wu, J., & Ye, W. (2018). Role of the mid-Holocene environmental transition in the decline of late Neolithic cultures in the deserts of NE China. *Quaternary Science Reviews*, *190*, 98–113. https://doi.org/10.1016/j.quascirev.2018.04.017

Gutiérrez Elorza, M., & Sesé Martínez, V. H. (2001). Multiple talus flatirons, variations of scarp retreat rates and the evolution of slopes in Almazán Basin (semi-arid central Spain). *Geomorphology*, *38*(1), 19–29. https://doi.org/10.1016/S0169-555X(00)00051-9

Han, T., Yu, K., Yan, H., Yan, H., Tao, S., Zhang, H., et al. (2019). The decadal variability of the global monsoon links to the North Atlantic climate since 1851. *Geophysical Research Letters*, *46*(15), 9054–9063. https://doi.org/10.1029/2019gl081907

Hathorne, E. C., Gagnon, A., Felis, T., Adkins, J., Asami, R., Boer, W., et al. (2013). Interlaboratory study for coral Sr/Ca and other element/Ca ratio measurements. *Geochemistry, Geophysics, Geosystems*, *14*(9), 3730–3750. https://doi.org/10.1002/ggge.20230

Hu, J., Emile-Geay, J., Tabor, C., Nusbaumer, J., & Partin, J. (2019). Deciphering oxygen isotope records from Chinese speleothems with an isotope-enabled climate model. *Paleoceanography and Paleoclimatology*, *34*(12), 2098–2112. https://doi.org/10.1029/2019PA003741

Jiang, H., Muscheler, R., Björck, S., Seidenkrantz, M.-S., Olsen, J., Sha, L., et al. (2015). Solar forcing of Holocene summer sea-surface temperatures in the northern North Atlantic. *Geology*, *43*(3), 203–206. https://doi.org/10.1130/g36377.1

Jing, Z.-y., Qi, Y.-q., Hua, Z.-l., & Zhang, H. (2009). Numerical study on the summer upwelling system in the northern continental shelf of the South China Sea. *Continental Shelf Research*, *29*(2), 467–478. https://doi.org/10.1016/j.csr.2008.11.008

Jouzel, J., Masson-Delmotte, V., Cattani, O., Dreyfus, G., Falourd, S., Hoffmann, G., et al (2007). Orbital and millennial Antarctic climate variability over the past 800,000 years. *Science*, *317*(5839), 793–796. https://doi.org/10.1126/science.1141038

Keigwin, L. D., & Boyle, E. A. (2000). Detecting Holocene changes in thermohaline circulation. *Proceedings of the National Academy of Sciences*, *97*(4), 1343–1346. https://doi.org/10.1073/pnas.97.4.1343

Knutson, D. W., Buddemeier, R. W., & Smith, S. V. (1972). Coral chronometers: seasonal growth bands in reef corals. *Science*, *177*(4045), 270–272. https://doi.org/10.1126/science.177.4045.270

Kobashi, T., Kawamura, K., Severinghaus, J. P., Barnola, J.-M., Nakaegawa, T., Vinther, B. M., et al. (2011). High variability of Greenland surface temperature over the past 4000 years estimated from trapped air in an ice core. *Geophysical Research Letters*, *38*(21). https://doi.org/10.1029/2011gl049444

Kobashi, T., Menviel, L., Jeltsch-Thommes, A., Vinther, B. M., Box, J. E., Muscheler, R., et al. (2017). Volcanic influence on centennial to millennial Holocene Greenland temperature change. *Scientific Reports*, *7*,1–10. https://doi.org/10.1038/s41598-017-01451-7

Kong, D., Zong, Y., Jia, G., Wei, G., Chen, M.-T., & Liu, Z. (2014). The development of late Holocene coastal cooling in the northern South China Sea. *Quaternary International*, *349*, 300–307. https://doi.org/10.1016/j.quaint.2013.08.055

Liu, X., Liu, J., Chen, S., Chen, J., Zhang, X., Yan, J., & Chen, F. (2020). New insights on Chinese cave δ^{18}O records and their paleoclimatic significance. *Earth-Science Reviews*, *207*, 103216. https://doi.org/10.1016/j.earscirev.2020.103216

Liu, Y., Peng, Z., Shen, C.-C., Zhou, R., Song, S., Shi, Z., et al. (2013). Recent 121-year variability of western boundary upwelling in the northern South China Sea. *Geophysical Research Letters*, *40*(12), 3180–3183. https://doi.org/10.1002/grl.50381

Lough, J. M. (2010). Climate records from corals. *Wires Clim Change*, *1*(3), 318–331. https://doi.org/10.1002/wcc.39

Ludwig, K. R. (2012). User's manual for Isoplot 3.75: A geochronological toolkit for Microsoft Excel. *Berkeley Geochronology Center Special Publication*, *5*, 1–75. http://www.bgc.org/isoplot_etc/isoplot.html

Mayewski, P. A., Rohling, E. E., Curt Stager, J., Karlén, W., Maasch, K. A., David Meeker, L., et al. (2004). Holocene climate variability. *Quaternary Research*, *62*(3), 243–255. https://doi.org/10.1016/j.yqres.2004.07.001

McCulloch, M. T., Gagan, M. K., Mortimer, G. E., Chivas, A. R., & Isdale, P. J. (1994). A high-resolution Sr/Ca and δ^{18}O coral record from the Great Barrier Reef, Australia, and the 1982-1983 El Niño. *Geochimica et Cosmochimica Acta*, *58*(12), 2747–2754. https://doi.org/10.1016/0016-7037(94)90142-2

Michaud, J. (1997). From Southwest China into Upper Indochina: an overview of Hmong (Miao) migrations. *Asia Pacific Viewpoint*, *38*(2), 119–130. https://doi.org/10.1111/1467-8373.00034

Morley, A., Rosenthal, Y., & deMenocal, P. (2014). Ocean-atmosphere climate shift during the mid-to-late Holocene transition. *Earth and Planetary Science Letters*, *388*, 18–26. https://doi.org/10.1016/j.epsl.2013.11.039

Nakamura, T., Masuda, K., Miyake, F., Hakozaki, M., Kimura, K., Nishimoto, H., & Hitoki, E. (2016). High-precision age determination of Holocene samples by radiocarbon dating with accelerator mass spectrometry at Nagoya University. *Quaternary International*, *397*, 250–257. https://doi.org/10.1016/j.quaint.2015.04.014

Nurhati, I. S., Cobb, K. M., Charles, C. D., & Dunbar, R. B. (2011). Correction to "Late 20th century warming and freshening in the central tropical Pacific". *Geophysical Research Letters*, *38*(24). https://doi.org/10.1029/2011gl049972

Okai, T., Suzuki, A., Kawahata, H., Terashima, S., & Imai, N. (2002). Preparation of a new Geological Survey of Japan geochemical reference material: Coral JCp-1. *Geostandard Newslett*, *26*(1), 95–99. https://doi.org/10.1111/j.1751-908X.2002.tb00627.x

Pearson, C. L., Brewer, P. W., Brown, D., Heaton, T. J., Hodgins, G. W. L., Jull, A. J. T., et al. (2018). Annual radiocarbon record indicates 16th century BCE date for the Thera eruption. *Science Advances*, *4*(8) eaar8241. https://doi.org/10.1126/sciadv.aar8241

Pfeiffer, M., Dullo, W.-C., Zinke, J., & Garbe-Schönberg, D. (2009). Three monthly coral Sr/Ca records from the Chagos Archipelago covering the period of 1950–1995 A.D.: reproducibility and implications for quantitative reconstructions of sea surface temperature variations. *International Journal of Earth Sciences*, *98*(1), 53–66. https://doi.org/10.1007/s00531-008-0326-z

Rahmstorf, S. (1994). Rapid climate transitions in a coupled ocean–atmosphere model. *Nature*, *372*(6501), 82–85. https://doi.org/10.1038/372082a0

Saraswat, R., Naik, D. K., Nigam, R., & Gaur, A. S. (2016). Timing, cause and consequences of mid-Holocene climate transition in the Arabian Sea. *Quaternary Research*, *86*(2), 162–169. https://doi.org/10.1016/j.yqres.2016.06.001

Sevink, J., van Bergen, M. J., van der Plicht, J., Feiken, H., Anastasia, C., & Huizinga, A. (2011). Robust date for the Bronze Age Avellino eruption (Somma-Vesuvius): 3945 ± 10 calBP (1995 ± 10 calBC). *Quaternary Science Reviews*, *30*(9), 1035–1046. https://doi.org/10.1016/j.quascirev.2011.02.001

Shi, N., & Zhu, Q. (1996). An abrupt change in the intensity of the East Asian summer monsoon index and its relationship with temperature and precipitation over east china. *International Journal of Climatology*, *16*(7), 757–764. https://doi.org/10.1002/(sici)1097-0088(199607)16:7<757::aid-joc50>3.0.co;2–5

Siklósy, Z., Demény, A., Vennemann, T. W., Kramers, J., Lauritzen, S. E., & Leél-Őssy, S. (2007). Middle bronze age climate change recorded in a Hungarian stalagmite: Triggering by volcanic activity?. *Paper presented at European Geosciences Union General Assembly 2007*. Vienna: Austria.

Siklósy, Z., Demény, A., Vennemann, T. W., Pilet, S., Kramers, J., Leél-Őssy, S., et al. (2009). Bronze Age volcanic event recorded in stalagmites by combined isotope and trace element studies. *Rapid Communications in Mass Spectrometry*, *23*(6), 801–808. https://doi.org/10.1002/rcm.3943

Song, S. H., Zhou, W. J., Peng, Z. C., Liu, W. G., Cheng, P., & Xian, F. (2006). Response to environmental conditions of coral d^{18}O of *Porites lutea* from Shalao, Hainan Island. *Marine Geology & Quaternary Geology*, *26*(4), 23–28. https://doi.org/10.16562/j.cnki.0256-1492.2006.04.004 (in Chinese with English abstract)

Staubwasser, M., Sirocko, F., Grootes, P. M., & Segl, M. (2003). Climate change at the 4.2 ka BP termination of the Indus valley civilization and Holocene South Asian monsoon variability. *Geophysical Research Letters*, *30*(8). https://doi.org/10.1029/2002gl016822

Steinhilber, F., Beer, J., & Fröhlich, C. (2009). Total solar irradiance during the Holocene. *Geophysical Research Letters*, *36*(19). https://doi.org/10.1029/2009GL040142

Steinke, S., Chiu, H.-Y., Yu, P.-S., Shen, C.-C., Erlenkeuser, H., Löwemark, L., & Chen, M.-T. (2006). On the influence of sea level and monsoon climate on the southern South China Sea freshwater budget over the last 22,000 years. *Quaternary Science Reviews*, *25*(13), 1475–1488. https://doi.org/10.1016/j.quascirev.2005.12.008

Stott, L., Cannariato, K., Thunell, R., Haug, G. H., Koutavas, A., & Lund, S. (2004). Decline of surface temperature and salinity in the western tropical Pacific Ocean in the Holocene epoch. *Nature*, *431*(7004), 56–59. https://doi.org/10.1038/nature02903

Vollweiler, N., Scholz, D., Mühlinghaus, C., Mangini, A., & Spötl, C. (2006). A precisely dated climate record for the last 9 kyr from three high alpine stalagmites, Spannagel Cave, Austria. *Geophysical Research Letters*, *33*(20), L20703. https://doi.org/10.1029/2006GL027662

Wang, B. (2006). *The Asian monsoon*. Berlin, Heidelberg: Springer-Verlag.

Wang, Y., Cheng, H., Edwards, R. L., He, Y., Kong, X., An, Z., et al. (2005). The Holocene Asian monsoon: Links to solar changes and north Atlantic climate. *Science*, *308*(5723), 854–857. https://doi.org/10.1126/science.1106296

Wang, X., Deng, W., Liu, X., Wei, G., Chen, X., Zhao, J.-x., et al. (2018). Super instrumental El Niño events recorded by a Porites coral from the South China Sea. *Coral Reefs*, *37*(1), 295–308. https://doi.org/10.1007/s00338-018-1658-1

Wanner, H., Beer, J., Bütikofer, J., Crowley, T. J., Cubasch, U., Flückiger, J., et al. (2008). Mid- to Late Holocene climate change: an overview. *Quaternary Science Reviews*, *27*(19), 1791–1828. https://doi.org/10.1016/j.quascirev.2008.06.013

Wanner, H., Solomina, O., Grosjean, M., Ritz, S. P., & Jetel, M. (2011). Structure and origin of Holocene cold events. *Quaternary Science Reviews*, *30*(21), 3109–3123. https://doi.org/10.1016/j.quascirev.2011.07.010

Weiss, H., Courty, M. A., Wetterstrom, W., Guichard, F., Senior, L., Meadow, R., & Curnow, A. (1993). The genesis and collapse of third millennium north Mesopotamian civilization. *Science*, *261*(5124), 995–1004. https://doi.org/10.1126/science.261.5124.995

Wu, W., & Ge, Q. (2005). The possibility of occurring of the extraordinary floods on the eve of establishment of the Xia Dynasty and the historical truth of Dayu's successful regulating of floodwaters. *Quaternary Sciences*, *25*(6), 741–749 (in Chinese with English abstract)

Wu, Q., Zhao, Z., Liu, L., Granger, D. E., Wang, H., Cohen, D. J., et al. (2016). Outburst flood at 1920 BCE supports historicity of China's Great Flood and the Xia dynasty. *Science*, *353*(6299), 579–582. https://doi.org/10.1126/science.aaf0842

Yancheva, G., Nowaczyk, N. R., Mingram, J., Dulski, P., Schettler, G., Negendank, J. F. W., et al. (2007). Influence of the intertropical convergence zone on the East Asian monsoon. *Nature*, *445*(7123), 74–77. https://doi.org/10.1038/nature05431

Yan, S., Zhao, J.-x., Lau, A. Y. A., Roff, G., Leonard, N. D., Clark, T. R., et al. (2019). Episodic Reef Growth in the Northern South China Sea linked to Warm Climate during the past 7,000 years: Potential for future coral Refugia. *Journal of Geophysical Research: Biogeosciences*, *124*(4), 1032–1043. https://doi.org/10.1029/2018jg004939

Ye, F., Deng, W., Xie, L., Wei, G., & Jia, G. (2014). Surface water δ18O in the marginal China seas and its hydrological implications. *Estuarine, Coastal and Shelf Science*, *147*, 25–31. https://doi.org/10.1016/j.ecss.2014.05.033

Yi, D. L., Melnichenko, O., Hacker, P., & Potemra, J. (2020). Remote sensing of sea surface salinity variability in the South China Sea. *Journal of Geophysical Research: Oceans*, *125*(12), e2020JC016827. https://doi.org/10.1029/2020JC016827

Yokoyama, Y., Suzuki, A., Siringan, F., Maeda, Y., Abe-Ouchi, A., Ohgaito, R., et al. (2011). Mid-Holocene palaeoceanography of the northern South China Sea using coupled fossil-modern coral and atmosphere-ocean GCM model. *Geophysical Research Letters*, *38*(8) L00F03. https://doi.org/10.1029/2010GL044231

Yu, K. (2012). Coral reefs in the South China Sea: Their response to and records on past environmental changes. *Science China Earth Sciences*, *55*(8), 1217–1229. https://doi.org/10.1007/s11430-012-4449-5

Yu, K. B., Kong, D.-Y., Lee, H. A., Kim, C. W., & Yim, J. S. (2016). Asian Monsoon Variation revealed by the speleothem records from Pyeongchang, Korea. *The Korean Association of Regional Geographers*, *22*(2), 439–449.

Zeng, L., Chassignet, E. P., Schmitt, R. W., Xu, X., & Wang, D. (2018). Salinification in the South China Sea since late 2012: A reversal of the freshening since the 1990s. *Geophysical Research Letters*, *45*(6), 2744–2751. https://doi.org/10.1002/2017GL076574

Zhang, P., Cheng, H., Edwards, R. L., Chen, F., Wang, Y., Yang, X., et al. (2008). A test of climate, sun, and culture relationships from an 1810-year Chinese cave record. *Science*, *322*(5903), 940–942. https://doi.org/10.1126/science.1163965

Zhang, L., Delworth, T. L., & Zeng, F. (2017). The impact of multidecadal Atlantic meridional overturning circulation variations on the Southern Ocean. *Climate Dynamics*, *48*(5), 2065–2085. https://doi.org/10.1007/s00382-016-3190-8

Zhang, Y., Zhu, K., Huang, C., Kong, D., He, Y., Wang, H., et al. (2019). Asian winter monsoon imprint on Holocene SST changes at the northern coast of the South China Sea. *Geophysical Research Letters*, *46*(22), 13363–13370. https://doi.org/10.1029/2019GL085617

Zhou, H., Zhao, J., Qing, W., Feng, Y., & Tang, J. (2011). Speleothem-derived Asian summer monsoon variations in Central China, 54–46ka. *Journal of Quaternary Science*, *26*(8), 781–790. https://doi.org/10.1002/jqs.1506

Zinke, J., Reuning, L., Pfeiffer, M., Wassenburg, J. A., Hardman, E., Jhangeer-Khan, R., et al. (2016). A sea surface temperature reconstruction for the southern Indian Ocean trade wind belt from corals in Rodrigues Island (19° S, 63° E). *Biogeosciences*, *13*(20), 5827–5847. https://doi.org/10.5194/bg-13-5827-2016